European Polymer Journal 49 (2013) 3548–3560

Contents lists available at ScienceDirect

European Polymer Journal

journal homepage: www.elsevier.com/locate/europolj

Chemical shrinkage and thermomechanical characterization of an epoxy resin during cure by a novel in situ measurement method

C. Billotte, F.M. Bernard, Edu Ruiz *

Chaire sur les Composites à Haute Performance (CCHP), École Polytechnique de Montréal, CP 6079, Centre-ville Station, Montreal, Quebec H3C 3A7, Canada

ARTICLE INFO

Article history:
Received 30 March 2012
Received in revised form 27 June 2013
Accepted 3 July 2013
Available online 6 August 2013

Keywords:
DMA
Calorimetry
Chemorheology
Mechanical properties
Curing
Thermosets characterization

ABSTRACT

In this study, a novel technique is presented to enable the characterization of the dimensional changes and evolution of mechanical properties of a resin during cure. This is achieved using an innovative in situ device called thermal flux cell combined with a Dynamical Mechanical thermal Analyser (DMA). With this system, it is now possible to eliminate the sources of error induced while combining two or more instruments. This device consists into a mold containing the resin where the upper and lower surfaces acting as heat flux sensors. Changes in temperature and thermal flux are directly monitored as well as the dynamical displacement and the stiffness during the curing process. In this work, an epoxy DGEBA resin was used to demonstrate the innovative approach. The tested resin was characterized using different vibration frequencies and amplitudes of the DMA. The results were then processed in order to provide accurate data on gel time and cure kinetics behavior. The volume and mechanical changes were also derived from experimental data and linked to the degree of cure. Chemo and thermo-mechanical models were created to predict the changes in chemical shrinkage and stiffness during cure.

© 2013 Elsevier Ltd. All rights reserved.

1. Introduction

As the composite industry grows, the use of thick parts and pieces of complex shape is increasingly in demand. Composite components for structural applications require larger cross-sections to respond to high mechanical stresses in contrast to shell-like composites used for semi or non-structural applications. The curing of thick parts remains a challenge because of their low thermal conductivity and the high heat of reaction generated during polymerization. This combination of low conductivity and high heat sources in the part can induce large temperature gradients, thus generation of internal stresses and possible polymer degradation. In order to improve the quality of thick composites, processing temperatures need to be well controlled to minimize the thermal gradients throughout the part. Moreover, the chemorheology and cure kinetics at high temperature are very different from what is observed at low temperature [1]. The reinforcing fibers are not affected during the process cycle, but the polymer matrix can shrink during cross-linking by as much as 10% [1,2]. During curing and consolidation, these different thermal behaviors induce internal stresses which can generate defects in the part affecting its mechanical performance and inducing geometrical distortions [2]. The resin gelation and vitrification as well as the chemical shrinkage have to be characterized in order to predict the geometrical variations of the part during processing and use.

The volumetric changes of thermoset resins during the curing process can be described as a combination between thermal effect due to expansion/contraction and chemical effect associated to the chemical shrinkage of the polymer chains [3]. The chemical shrinkage takes place during the formation of the polymer network [4] and results from the movement in the molecule from Van der Waals

* Corresponding author. Tel.: +1 514 340 4711; fax: +1 514 340 5867.
E-mail address: edu.ruiz@polymtl.ca (E. Ruiz).

0014-3057/$ - see front matter © 2013 Elsevier Ltd. All rights reserved.
http://dx.doi.org/10.1016/j.eurpolymj.2013.07.013

bonding distance in monomer to covalent bonding distance when polymer was formed [5,6]. These volumetric changes during processing can generate several defects such as bad surface appearance, waviness, spring-in/spring-back, dimensional inaccuracy and more, leading to a decrement of the part quality and performance [7].

In the past, different methods have been developed for the shrinkage measurement including ASTM D2566 standard which is based on volume measurement before and after cure. However this method underestimates the shrinkage since it does not take into account the thermal effects during cure. Techniques for shrinkage measurements can be mainly divided into two approaches: direct methods such as volumetric dilatometry or indirect methods which measure the linear shrinkage and rely on assumptions to calculate the volumetric shrinkage. In the first category, among the most common methods are the capillary dilatometry [3,5] and Pressure–Volume–Temperature (PVT) device [8,9]. Numerous techniques belong to the second category such as gravimetric method [3,10,11] based on the Archimedean principle, Thermo Mechanical Analysis (TMA) [6,12], Dynamic Mechanical Analysis (DMA) [13] and rheology [10,14]. However, most of these methods require coupled characterization with a calorimeter to associate the shrinkage with the degree of cure (DoC) [12]. This generates numerous errors due to time lag caused by measurement techniques and differences on the size of the samples used on each technique.

In this study, a novel technique is presented which allows simultaneous characterization of resin cure, as well as of dimensional and rheological changes that take place during polymerization. These characterizations are performed with an innovative thermal flux cell combined with a Dynamical Mechanical thermo Analyzer (DMA) apparatus. Changes in temperature and thermal fluxes are directly monitored as well as the volume and stiffness variations of the sample during processing. The experimental data were processed in order to provide accurate data on gel time and cure kinetics. The dimensional and mechanical changes were linked to the degree of cure. Chemorheological models were then created to predict the physical behavior of the resin, leading to further optimization of the manufacturing of composite parts. This innovative approach allows multiple characterization of the polymer matrix during processing reducing the complex and time consuming task of combining data from different instruments. Moreover, this technique also allows characterization of the composite laminate in the same fixture. This has the advantage of bringing key information for component design.

2. Experimental

2.1. Heat flux cell

The thermal, shrinkage and dynamic mechanical measurements were carried out with a Dynamical Mechanical thermal Analyzer DMA + 450 from Metravib. In this work, a new fixture named "heat flux cell" was developed to make possible the combined measurements. The heat flux cell is illustrated in Fig. 1 and consists of two upper and lower plates with a cavity between them to hold the sample. This novel heat flux cell enables direct injection of the liquid resin into a closed cavity. The temperature control is ensured by the thermal enclosure of the DMA instrument. The resin is contained in the mold where the upper and lower surfaces act as heat flux sensors. A Teflon ring covers the two plates to provide insulation of the sample to its surrounding to minimize side thermal effects.

The heat flux and temperature signals are directly monitored by the area heat flux sensors, which deliver electrical signal proportional to heat flux density (W/m^2) passing through them. The heat flux cell is calibrated with a calibrated electric heater. These sensors and calibrated heater are provided by Thermoflux. Sample shrinkage and stiffness result are respectively from the dynamic load and displacement of the DMA instrument. The dynamic solicitation is processed to a voltage generator and a power amplifier, than the signal is transmitted to an electrodynamic exciter (magnetic circuit and exciting coils). The signal is analyzed by a dynamic displacement sensor and piezoelectric force sensor. Mechanical properties can then be derived from the stiffness response, which is the raw measured signal of the DMA. The shrinkage measurement principle is somewhat similar to the rheological method developed by Haider et al. [14], which is based on the measurement of the gap variation between two parallel plates with a normal force control. However, in this case the contact between the sample and the head of the DMA device is ensured by dynamic oscillation. The gap between the upper and lower plates is controlled by the displacement of the mobile head of the DMA. A thin layer of demolding agent is sprayed on the sample holders for the removal of the cured resin.

2.2. Heat of reaction and degree of cure

The instantaneous heat $\dot{H}$ generated during the cross-linking reaction of the polymer can be determined by the following equation [12,15,16]:

$$\dot{H} = \frac{dH}{dt} = H_T \frac{d\alpha}{dt} \tag{1}$$

where H_T is the total heat of reaction during cure and $d\alpha/dt$ the reaction rate. If the diffusion of chemical species is neglected and the reaction rate is assumed to be a unique function of the degree of conversion α and temperature T, this expression can take the following form:

$$\frac{d\alpha}{dt} = f(T,\alpha) \quad \text{and} \quad \alpha = \int_0^t \frac{d\alpha}{dt} \tag{2}$$

The total heat of reaction H_T corresponds to the area under the heat flux curve measured during cure [12]:

$$H_T = \int_0^t h(t)dt \tag{3}$$

where $h(t)$ is the specific heat flux measured by the instrument. However, during cure, changes may occur in heat capacity C_p and these variations can be seen in the thermal baseline [12]. This should be subtracted from the

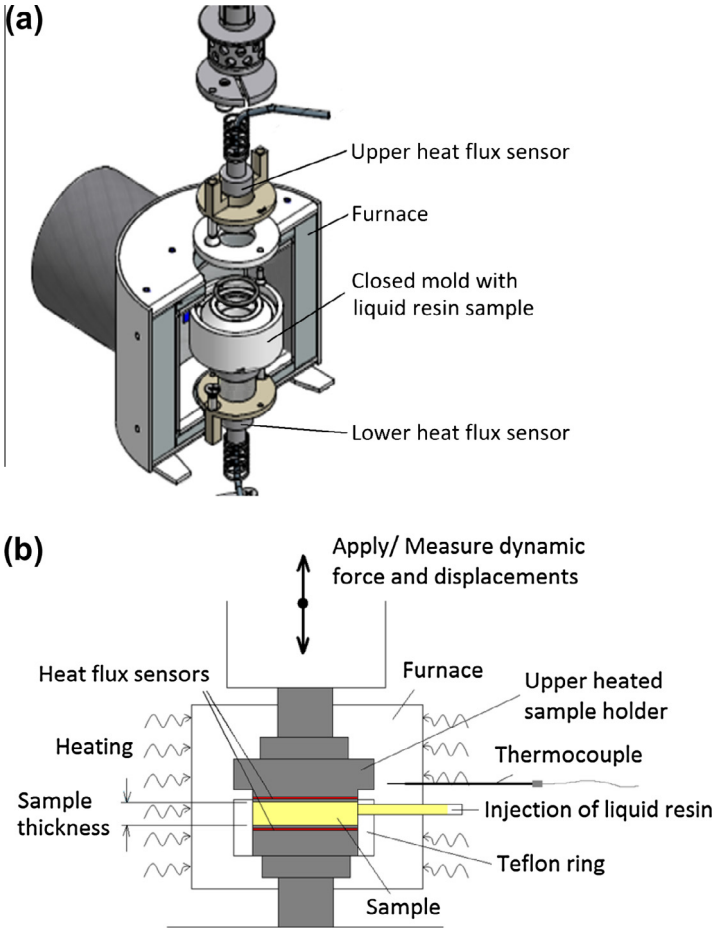

Fig. 1. Thermal flux cell HFC200 on DMA + 450: (a) design of the fixture and (b) working principle.

instrument signal before integration in order to get only the raw cure kinetic signal:

$$h(t) = h(t)_{\text{measured}} - h(t)_{\text{baseline}} \tag{4}$$

By solving Eq. (1), the reaction rate is defined by the specific heat flux divided by the total heat of reaction:

$$\frac{d\alpha}{dt}(t) = \frac{h(t)}{H_T} \tag{5}$$

The instantaneous degree of cure $\alpha(t)$ is derived from the curve as the ratio of the instant heat released over the total reaction enthalpy H_T:

$$\alpha(t) = \frac{1}{H_T}\int_0^t h(t)dt \tag{6}$$

When the reaction is completed, the ultimate degree of cure reached is calculated over the entire range of the exothermic peak and denoted α_{ult}. In the novel characterization cell described in this work, the heat of reaction was measured with the heat flux sensors in close contact with the sample. The heat of reaction was computed as the average heat flow measured at the upper plus the lower plates of the cell.

2.3. Material and experimental set up

The resin system used in this study is a Diglycidyl Ether of Bisphenol A (DGEBA) epoxy–anhydride resin system. The mixing of resin and hardener was prepared in larger quantity (about 100 g) than required for testing in order to ensure proper mixing. For isothermal tests, the temperature of the chamber is stabilized before injecting the liquid resin into the cell with a syringe. Data are monitored from the stabilization period, before resin injection, to keep track of the first events that take place after injection. In this work, three sets of experiments were performed, labeled series A, B and C as summarized in Tables 1–3. The tests from series A (see Table 1) were used to define the quantity of resin to be injected and therefore the adjustment of the initial distance between the lower and upper plates of the sample holder. Different strain amplitudes (A) and frequencies (f) were also tested for dynamic loading. The tests from series B (see Table 2) were all performed at the optimized sample volume of 2 mL obtained from series A, which corresponds to a mass (m) of around 0.90 g. The gap between plates was adjusted to 2 mm and the strain amplitude and frequency were respectively set to 20 μm and 10 Hz for this series of experiments.

Table 1
Heat of reaction H_T, linear shrinkage S_h and stiffness K of fully cured epoxy–anhydride resin system of series A.

Sample	A (μm)	f (Hz)	m (g)	H_T (J/g)	S_h (%)	K (×10 MN/m)	ΔT (°C)
A-1	20	10	0.6733	370.15	2.43	2.28	3.8
A-2	20	10	0.9782	355.55	2.75	2.64	5.8
A-3	20	10	0.8724	372.52	2.00	2.33	5.3
A-4	20	10	0.9498	356.22	2.55	2.35	4.7
A-5	20	10	0.9460	353.51	2.97	3.34	5.3
A-6	20	10	0.5268	335.86	2.48	3.21	3
A-7	20	10	1.0822	394.68	3.44	2.45	7.7
A-8	20	10	1.0900	345.52	3.42	2.43	5.8
A-9	40	10	1.2200	384.85	3.37	2.37	7.8
A-10	40	10	0.5151	346.51	2.43	2.48	3.8
A-11	5	10	0.3580	360.03	2.35	1.85	1.8
A-12	5	10	0.9540	341.15	2.59	2.45	8.2
A-13	5	10	0.8660	336.98	2.13	2.46	4
A-14	5	10	1.1300	355.66	2.98	2.46	7.4
A-15	2	10	0.3255	347.47	1.09	1.01	1.5
A-16	2	10	0.8770	355.35	2.03	2.46	5.4
Average	**–**	**–**	**–**	**357.00**	**2.56**	**2.41**	**–**
St dev	**–**	**–**	**–**	**16.47**	**0.61**	**0.51**	**–**

Table 2
Heat of reaction H_T, linear shrinkage S_h and stiffness K of fully cured epoxy–anhydride resin system of series B (A = 20 μm and f = 10 Hz).

Sample	m (g)	H_T (J/g)	S_h (%)	K (×10 MN/m)
B-1	0.8814	332.79	3.04	2.49
B-2	0.9183	344.82	3.02	2.31
B-3	0.8980	315.37	2.99	2.32
B-4	0.9651	392.26	3.03	2.53
B-5	0.9302	315.65	2.52	2.52
B-6	0.9236	353.72	2.91	2.52
B-7	0.8756	298.40	2.90	2.28
B-8	0.7810	306.88	2.90	2.50
B-9	0.7512	317.40	2.47	1.61
B-10	1.0166	332.34	2.58	1.80
B-11	0.9351	320.79	2.86	2.19
B-12	0.9595	321.05	2.39	1.97
B-13	0.9581	310.26	2.82	2.44
Average	**0.9072**	**327.83**	**2.80**	**2.27**
St dev	**0.0732**	**24.62**	**0.23**	**0.30**

The tests of series C (see Table 3) were carried out to study the influence of the oscillation parameters on the resin characterization. To do so, dynamic strain amplitudes from 5 to 40 μm and frequencies from 1 to 100 Hz were explored. All tests were carried out at isothermal temperature of 120 °C.

For comparison purpose, Differential Scanning Calorimetry (DSC) experiments were conducted using TA Instruments Q1000 under similar isothermal conditions at 120 °C as the DMA tests and also with a heating ramp of 3 °C/min. Heat of reaction was calculated from the total heat flow curve. Gel point determination was also carried out using Anton-Paar MCR501 rheometer. Experiments were run under Small Amplitude Oscillatory Shear (SAOS) at strain of 1% and frequency of 50 rad/s. The choice of the strain amplitude was done in the linear viscoelastic (LVE) region.

3. Results and discussion

The first plan of experiments (series A) presented in Table 1 consist of a total of 16 runs carried out to optimize the testing parameters to be used for this characterization. The sample mass was varied from 0.36 to 1.2 g (i.e. 0.8–2.7 mL). Higher sample mass will generate more reaction energy and may induce changes on the measured heat of reaction as illustrated in Fig. 2a. On the other hand, a low

Table 3
Heat of reaction H_T, linear shrinkage S_h and stiffness K of fully cured epoxy–anhydride resin system of series C.

Sample	A (μm)	f (Hz)	m (g)	H_T (J/g)	S_h (%)	K (×10 MN/m)
C-1	20	1	0.9338	316.06	2.40	2.08
C-2	20	1	0.8901	317.34	2.83	2.23
C-3	20	1	0.8142	328.99	2.49	2.19
C-4	20	1	0.9008	316.85	2.57	2.16
C-5	20	100	0.7666	325.92	2.41	2.45
C-6	20	100	0.8140	313.35	2.36	2.36
C-7	20	100	0.8396	324.02	2.21	2.40
C-8	40	100	0.9940	311.45	2.34	2.62
C-9	40	100	0.9298	317.56	1.98	2.47
C-10	5	100	0.9493	318.43	2.55	2.49
C-11	5	100	0.9939	308.30	2.63	2.49
Average	**–**	**–**	**0.8932**	**318.02**	**2.43**	**2.36**
St dev	**–**	**–**	**0.0761**	**6.20**	**0.22**	**0.17**

sample mass may not generate enough heat to properly measure the reaction specific enthalpy. However, from the results of series A, the reaction specific enthalpy seems not to be linked to the sample mass used on these tests. The averaged heat of reaction was of 357 J/g with a standard deviation of the mean of 16 J/g, which is acceptable for this characterization (see Table 1). The temperature increment during the exothermic reaction was affected by the sample mass (see Fig. 2b). For samples of less than 0.5 g, the temperature jump ΔT was of 2 °C while for sample of more than 1 g ΔT was of 6 °C. This indicates that increasing sample mass will induce a deviation of the isothermal cure condition. Based on these analyses, the sample mass was fixed to 0.9 g which corresponds to the volume of a cylindrical sample of 20 mm diameter and 2 mm thick. This series was also configured to evaluate the impact of oscillation amplitude on the measured shrinkage (*Sh*) and sample stiffness (*K*). However, no relationship was observed between mass of the sample and *Sh* or *K*.

The second plan of experiments, series B, was designed to evaluate the variability of the characterization when all parameters are kept constant. In this case, an average sample mass of 0.9 g (i.e. 2 mL) was injected into the pre-heated chamber. The frequency and amplitude of oscillation were both kept constant at 10 Hz and 20 μm

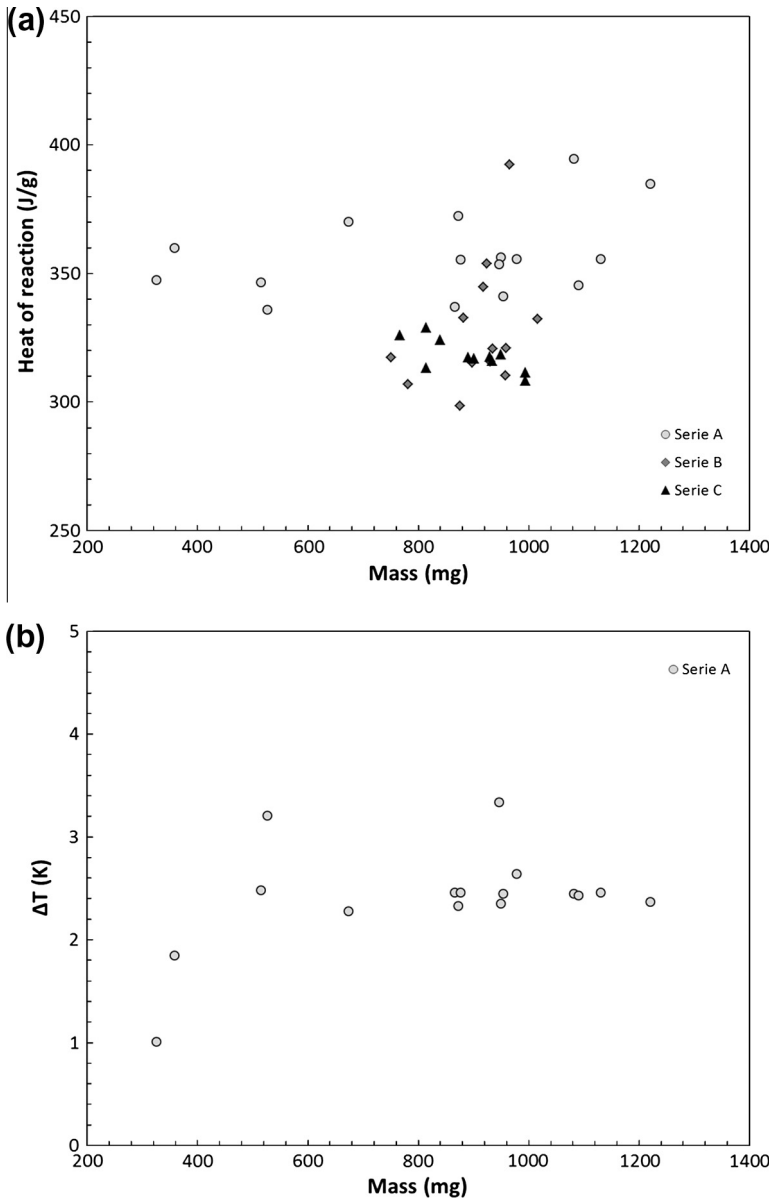

Fig. 2. Impact of sample mass: (a) on the measured heat of reaction and (b) temperature jump.

respectively. From the 13 tested samples, the standard deviation of the observations of the measured heat flow, shrinkage and stiffness was below 10% (see Table 2).

Fig. 3 shows an example of the evolution of the heat flux generated by the cross linking reaction of the epoxy–anhydride resin at 120 °C in the DMA. The sudden drop of heat at the beginning of the curve (i.e. values below zero) is due to the thermal shock created by the injection of the liquid resin at room temperature. During cross-linking, the two heat sensors record a positive change of the heat flux with a maximum peak reached around 300 s. The polymerization is completed after 1000 s as illustrated by the ending plateau. In order to get comparative basis between the samples, the measured heat flux is divided by the sample mass.

The heat of reaction of the epoxy resin was also measured using Differential Scanning Calorimetry (DSC) under the same temperature history as in the DMA heat flux cell. A modulated DSC Q1000 from TA Instruments [17,18] was used for this characterization. For comparison purpose, three samples of 8.5 ± 1 mg mass were isothermally cured at 120 °C. These tests were run over a period for 1000 s as the DMA tests. Additional tests were conducted in dynamic mode with a heating ramp of 3 °C/min. The average heat of reaction measured by DSC on these 20 experiments was 326 ± 6 J/g.

The heat of reaction of 337 ± 24 J/g reported in Table 4 is the resulting average of 40 experiments (series A, B and C combined) carried out on the DMA at similar thermal conditions. This result is in good agreement with the values obtained on the M-DSC instrument. However, the DMA cell shows higher dispersion than M-DSC. Variability between series is associated with sample dimension and mass under the flux sensors. The injection technique was also improved from one series to another resulting in a variation of sample volume and resin distribution on the sample holder.

Fig. 4 shows the evolution of the resin heat of reaction during cure at 120 °C. This heat of reaction was obtained by integration of curves in Fig. 3 following Eq. (3). A nearly full cure is obtained after 600 s although some heat still released until 1000 s. The cure behavior shown by samples B1 to B3 shows the variability of the technique. Fig. 5 shows the thermal history and cure evolution during an isothermal test on the DMA cell. Initially, the cell is kept isothermal at 120 °C. The resin is then injected at room temperature at 0 s, which is denoted by a drop of 1 °C in the temperature of the cell. The temperature of the system then increases due to the exothermic reaction of the resin. At 300 s, the reaction of the resin is enough to release sufficient heat to increase the temperature locally up to 124 °C. The degree of cure was obtained by integration of the heat flow (see Fig. 3) as presented in Eq. (6). At the exothermic peak, the resin undergoes a degree of cure of 70%, meaning that gelation has already occurred prior to 300 s. A full cure is observed after 1000 s. Additional explanation about gelation will be detailed further.

Table 4
Comparison of the heat of reaction of the epoxy–anhydride resin measured by DSC and the novel DMA HFC200 cell.

	DMA	DSC
Number of samples	40	20
Average H_T (J/g)	337	326
St dev (J/g)	24	6

Fig. 6 illustrates the evolution of degree of cure with time using both DMA cell and DSC methods. The degree of cure evaluated with the DSC technique (full line) arises before the DMA. For both experiments, the sample was maintained at room temperature and then injected or introduced in the device which was preheated at 120 °C. This time shift is not negligible and should therefore be compensated in the case of coupling measurements from different devices [12]. In Fig. 6, the DMA and DSC curves show a similar slope during most of the curing process. It is known that during isothermal cure experiments, variability may occur because of the temperature instabilities [19] and large difference in sample mass between

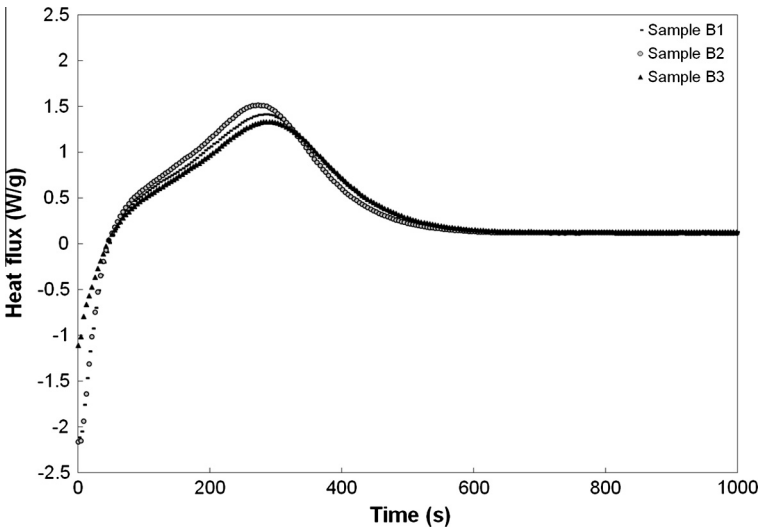

Fig. 3. Sample heat flux measured during isothermal cure of epoxy–anhydride resin at 120 °C with the novel DMA HFC200 cell for samples of series B.

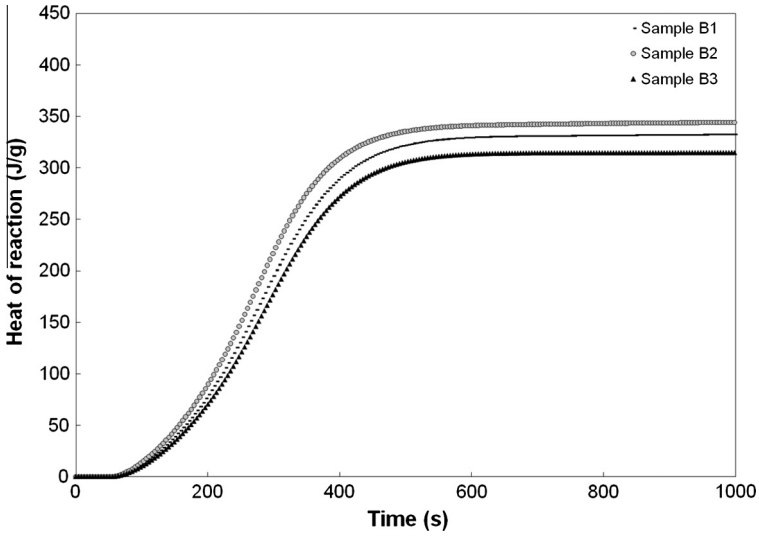

Fig. 4. Evolution of the heat of reaction with time during isothermal cure of epoxy–anhydride resin at 120 °C with the novel DMA HFC200 cell for samples of series B.

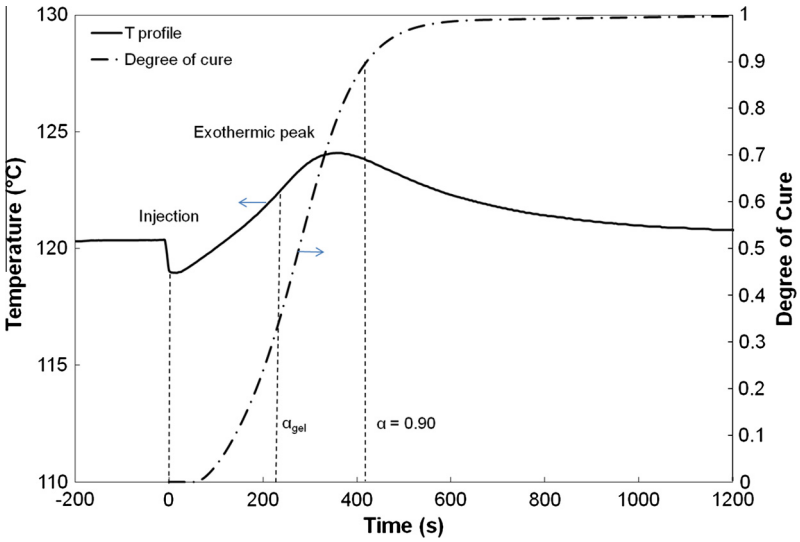

Fig. 5. Thermal history and cure evolution during isothermal test at 120 °C.

these two devices. Given that the sample mass is three orders of magnitude larger for the DMA test than the DSC, temperature gradients are expected to be a source of cure differences. As the cure reaction progresses, the resin becomes more solid reducing the mobility of the polymer chains. After 90% cure, the polymerization is mainly controlled by diffusion. At this point, the differences in sample mass between DSC and DMA will have an important impact on the cure process. This effect can be seen in Fig. 6 by the differences in slopes near the plateau at the end of cure.

3.1. Stiffness and resin shrinkage analysis and modeling

In the second experimental plan (series B in Table 2), the upper plate of the DMA cell oscillates at amplitudes of 20 μm and frequency of 10 Hz. The instrument applies a controlled force to induce such oscillation to the resin sample. As the liquid resin undergoes polymerization, the dynamic force required to apply a constant amplitude oscillation will increase from gelation to full cure. Then, knowing the variation on dynamic force, the change in mechanical properties of the resin can be followed during polymerization. On the other hand, when the resin shrinks during cure, the instrument adjusts the position of the upper plate so that it is in continuous contact with the sample (see Fig. 1). Measuring the static position of the upper plate is then a direct evaluation of the volume changes occurred during resin polymerization.

Fig. 7a illustrates the evolution of sample stiffness during resin cure on the DMA cell. At the early beginning of the test, the liquid resin has no dynamical mechanical

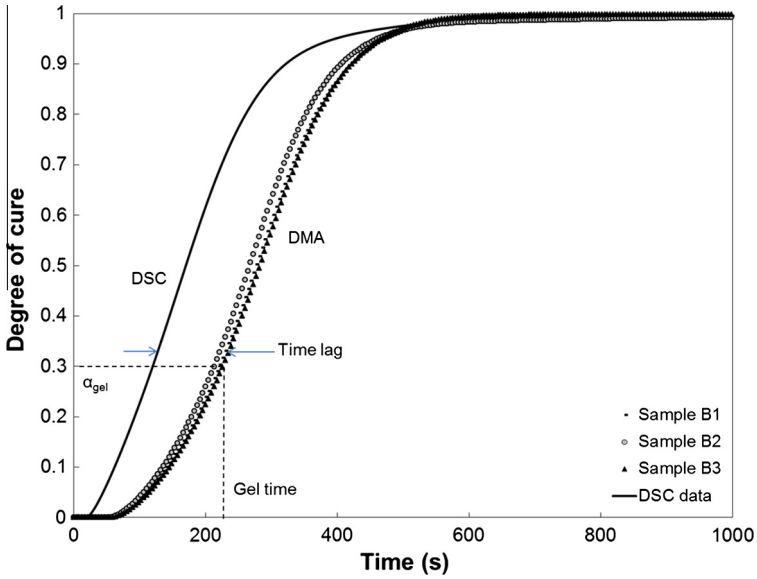

Fig. 6. Comparison between degree of cure measured with DSC and the DMA HCF200 cell for samples of series B.

properties and a stiffness of 10 N/m is measured by the DMA cell. This small stiffness is due to the moving liquid under dynamic compaction. The stiffness slowly increases linearly the first 200 s up to 50 N/m corresponding to 20% of cure. At this stage the polymer chains start to form an inter-connected tridimensional network resulting in a quick increment of mechanical properties shown by sudden change to a steeper slope in stiffness. Fig. 7a also shows the evolution of Tanδ which is the ratio between the storage and loss modulus of the dynamic stiffness. It can be seen that a maximum of Tanδ is observed at 230 s, representing a maximum of the dissipating energy in the sample. The peak in Tanδ can be associated to the initiation of resin gelation [20] and the time value from DMA test is quite close to the gel time of 245 s from rheology data as illustrated in Fig. 7b, considering the point that the instruments principle is quite different and cannot be compared on an absolute basis. This time of 245 s corresponds to the cross-over of the storage (G') and loss modulus (G'') and at this point the complex viscosity (η^*) starts to increase to infinity. Rheology gel point determination was verified for different frequencies from 5 to 100 rad/s and the gel time was found to be independent to frequency [21,22]. The difference of 15 s in the gel point detection between DMA and rheology can be associated to the difference in the measurement principle and sample mass inertia. As illustrated in Fig. 7a, at gel, the material changes from a liquid-like to a gel-like state and since it is no longer flowing, it reveals a pseudo-elastic behavior similar as a solid when compacted. The sample's mechanical properties grow logarithmically from this gelation point until reaching a plateau of 10^7 N/m at the end of cure.

In a previous work, Ruiz and Trochu [2,12] have model this non linear behavior with a log–log function of degree of cure. They have shown that the evolution of mechanical properties starts just after gelation and increases, following a logarithmic function, until the sample is fully cured. This non linear function of cure is assumed to be related to the increment of glass transition temperature (T_g) from the monomer to the polymer. The increment of T_g is a power law function of cure as described by Di Benedetto equation [23]. In this study, a new model is proposed to predict the evolution of mechanical properties with degree of cure as presented in the following equation.

$$\frac{\log K}{\log \alpha} \cong B \quad \text{and} \quad \log K = B\left[\frac{(1-\alpha_{gel})\log\alpha + 1}{(1-\alpha_{gel})}\right] \tag{7}$$

where K is the stiffness of the sample, α the degree of cure, B a fitting constant obtained from the experimental results and α_{gel} is the degree of cure at gelation (i.e. peak of Tanδ in Fig. 7). The first equation on the left represents the general trend by a log–log function, while the equation on the right is the particular model proposed for the epoxy-anhydride resin been studied. The parameters of this model are reported in Table 5.

Fig. 8 illustrates the evolution of stiffness during polymerization for samples of series B and C (see Tables 2 and 3) which was found to be nonlinear from the same degree of cure of 33% which corresponds to the gelation point. Although there are differences in stiffness before gelation, the data overlapped after gelation. This nonlinear relation was also reported by previous studies of Ruiz et al. [2,12] for polyester resins and more recently Abou Msallem et al. [24] for epoxy resins. These approaches take into account the transition from viscoelastic to elastic behavior and the glass transition temperature as well.

Along the polymerization, the upper plate of the sample-holder dynamically stimulates the resin with strain amplitude of 20 μm and frequency of 10 Hz. The position of the sample holder $z(t)$ is defined as the average value of the oscillation and a controller ensures that the dynamic displacement around this value is maintained at constant predefined amplitude. The variation in time of linear

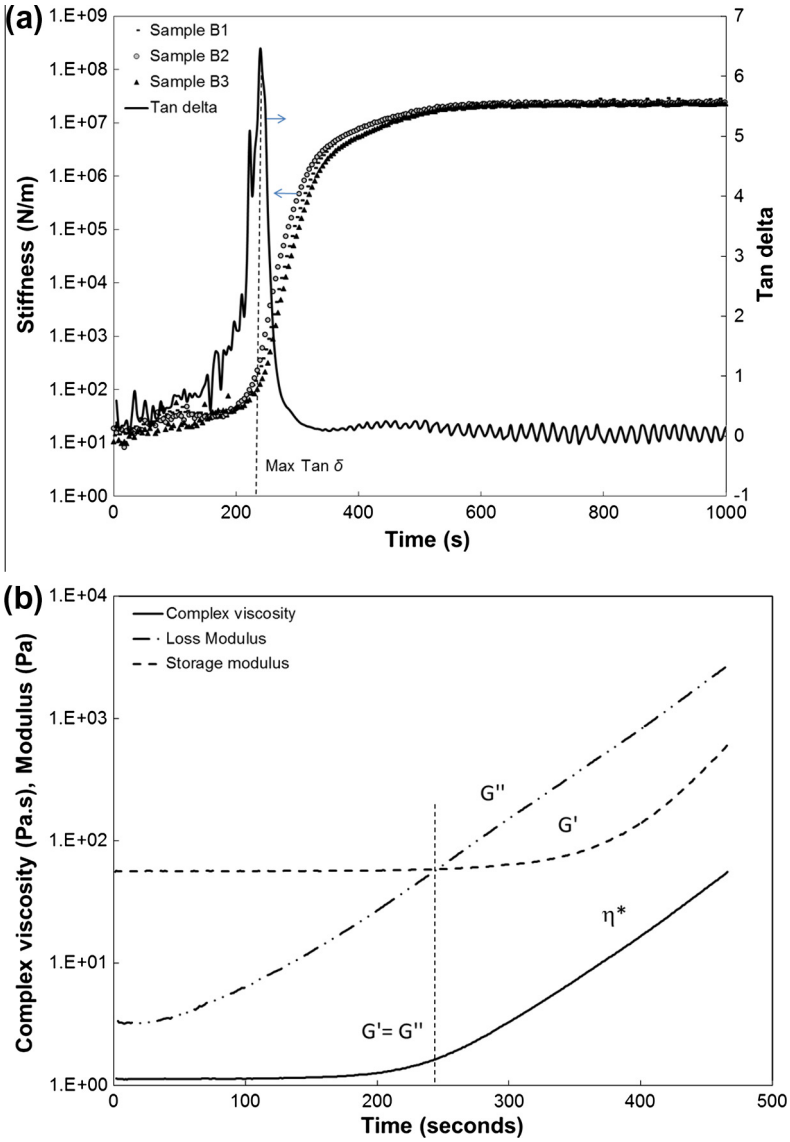

Fig. 7. Evolution of stiffness and rheology properties with time during isothermal cure of epoxy–anhydride resin at 120 °C: (a) evolution of stiffness and Tan δ for samples of series B during DMA experiment, (b) evolution of complex viscosity and storage and loss modulus during rheology SAOS experiment (1% strain amplitude, 50 rad/s frequency).

Table 5
Parameters of proposed models to predict stiffness and resin shrinkage during cure.

Stiffness model Eq. (7)		Shrinkage model Eq.(13)	
B	11.225	**C**	5.050
α_{gel}	0.332	α_c	0.535

shrinkage of the polymer $Sh(t)$ can then be defined as follows:

$$Sh(t) = \frac{z(t) - z_{init}}{th_{init}} \tag{8}$$

where z_{init} is the initial position of the upper plate of the sample holder (see Fig. 1), $z(t)$ is the varying position in time of the upper plate, and th_{init} is the initial thickness of the liquid sample. Given that the resin is at liquid state at the beginning of the experiment and therefore does not oppose sufficient resistance to the upper plate, some variations may occur at the early stages of the test. To overcome this issue, the reference position z_{init} is chosen after injection of the resin, once the displacement of the upper plate is stabilized. In this particular fixture, the DMA does not give direct information about the initial distance between the upper and lower plates defining the thickness of the liquid sample. Then, the initial thickness needs to be calculated taking into account the variation of the position of the upper plate of sample holder together with the final thickness of the cured sample which is measured. To obtain the initial thickness, a calculation was then carried

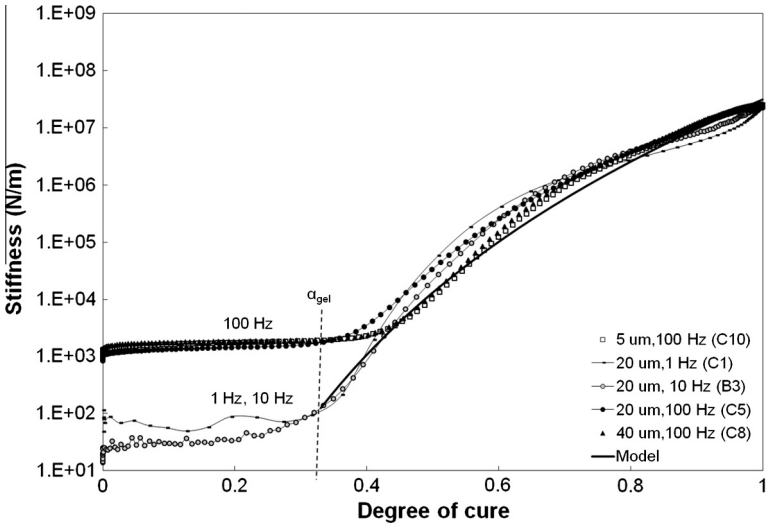

Fig. 8. Stiffness as a function of degree of cure and proposed model. Isothermal cure at 120 °C of epoxy–anhydride resin for samples of series B and C.

out from the final thickness of the sample and the measured shrinkage as follows:

$$th_{init} = th_{final} + \Delta z \quad \text{with} \quad \Delta z = |z_{final} - z_{init}| \tag{9}$$

where th_{final} is the measured final thickness of the cured sample and Δz the variation between the final (z_{final}) and initial (z_{init}) positions of the upper plate of the sample holder.

Previous experimental studies have been conducted by several researchers relating the volumetric changes that occur during thermoset processing. Hill et al. [3] proposed that the overall volumetric changes of a thermoset resin during cure can be considered as a combination between thermal expansion/contraction and polymerization shrinkage as follows:

$$\left(\frac{1}{V_0}\frac{dV}{dt}\right)_{\text{overall}} = \left(\frac{1}{V_0}\frac{dV}{dt}\right)_{\text{Thermal contribution}} - \left(\frac{1}{V_0}\frac{dV}{dt}\right)_{\text{Polymerization shrinkage}} \tag{10}$$

where the first term on the right-hand of Eq. (10) represents the bulk thermal expansion and contraction contribution and is expressed as follows:

$$\left(\frac{1}{V_0}\frac{dV}{dt}\right)_{\text{Thermal contribution}} = CTE\frac{dT}{dt} = \left[CTE_m(1-\alpha) + CTE_p\alpha\right]\frac{dT}{dt} \tag{11}$$

where CTE is the coefficient of volumetric thermal expansion with m and p suffixes referring to the monomer and

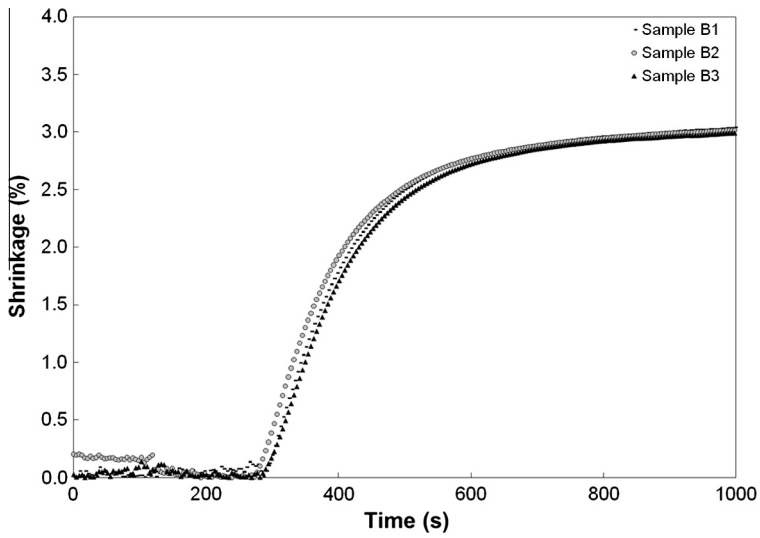

Fig. 9. Evolution of resin shrinkage with time during isothermal cure at 120 °C of epoxy–anhydride resin with the DMA HFC200 cell for samples of series B.

polymer states [3]. In this study, since tests were carried out under isothermal conditions, the volume changes due to thermal expansion were neglected to simplify. The second term of Eq. (10) represents the shrinkage associated to the chemical cure reaction. This latter was expressed by a simple linear relation between the shrinkage and the conversion and is assumed to be proportional to the reaction rate:

$$\left(\frac{1}{V_0}\frac{dV}{dt}\right)_{\text{Polymerization shrinkage}} = C\frac{d\alpha}{dt} \tag{12}$$

where C is a constant determined from the experimental results. In this work, chemical shrinkage was measured by the static displacement of the upper plate of the DMA cell during resin cure. As illustrated in Fig. 9, shrinkage is noticeable from 280 s, where the minimum stiffness of 100 N/m is reached. At this moment, the sample has already gellified and is seen to have noticeable shrinkage. It can be noticed that a delay appears between the gelation and the detection of mechanical properties and the beginning of the shrinkage at 280 s. This time difference is associated with the stage of the material between the beginning of gelation at 33% of cure and the rubbery-like material at 54% of cure when shrinkage is noticeable. During cure, the exothermic chemical reaction increases the sample temperature from 1 to 4 °C (see Fig. 5). As a consequence, the sample will expand and compensate shrinkage. The thermal expansion of liquid polymers is in the order of 35×10^{-5} m/m/°C [12]. For a 5 °C increment, the expansion of the sample would be below 0.2%. This quantity is much lower than the polymer shrinkage varying from 3% to 10% [4,6,10,25,26], thermal gradients can then be neglected on this study.

Fig. 10 shows the measured shrinkage as a function of degree of cure. The beginning of shrinkage is observed at 54% of cure. From this polymerization degree, the linear shrinkage increases proportionally until nearly full cure. This behavior is consistent with previous observations on thermoset resins [3,8,10,12,14,26] and can be modeled by the following equation:

$$l = C(\alpha - \alpha_c) \tag{13}$$

where l is the linear shrinkage, α the degree of cure at beginning of shrinkage and a α_c is a constant determined from the experimental results. The value of these model parameters for the epoxy-anhydride resin is reported in Table 5. This linear shrinkage behavior is observed until the polymerization reaches a DoC of 90%. At this point the cure reaction is controlled by thermal diffusivity and the deviation of the experimental points from the linear behavior can be associated to the non-negligible sample mass. Similar observations were reported in the past for a similar aeronautical epoxy resin [10]. However, no much explanation of this phenomenon is given. The maximum shrinkage attainable by the resin studied in this work is around 3% which is in the usual range of epoxies.

3.2. Validation of test parameters

In series B, the shrinkage and stiffness results presented so far were obtained at strain amplitude of 20 μm and frequency of 10 Hz. However, other combinations of frequency and amplitude were tested to validate these results. As presented in Table 3 (series C), the frequency of the dynamic load was varied from 1 to 100 Hz, while the amplitude of the excitation was increased from 5 to 40 μm. Fig. 8 shows the resulting stiffness when applying these test parameters. As it can be observed, when a frequency of 100 Hz is applied to the dynamic load, the initial stiffness of the sample increases by an order of magnitude of 1000 N/m. This is associated to a thickening phenomenon attributed to high frequency which is no longer in the linear viscoelastic domain of the material. However, this phenomenon seems to be independent of the oscillation amplitude.

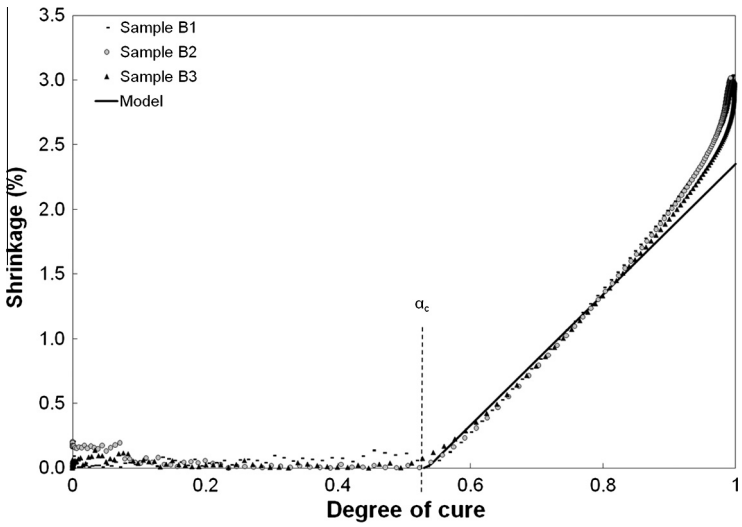

Fig. 10. Resin shrinkage as function of the degree of cure and proposed model. Isothermal cure at 120 °C of resin–anhydride resin with the DMA HFC200 cell for samples of series B.

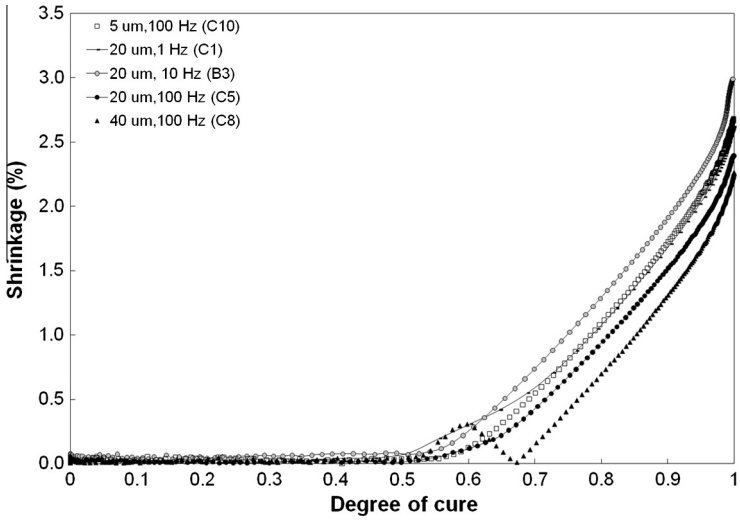

Fig. 11. Comparison between resin shrinkage measurements for different parameters configuration in dynamic displacement for samples of series B and C.

Fig. 11 shows the influence of varying the test parameters on the shrinkage measurement. The overall behavior of the shrinkage is not influenced by frequency or amplitude of the test. However, increasing the frequency to 100 Hz of amplitude to 40 μm delays the detection of shrinkage from 50% to 70% of cure. Based on these results it was concluded that the combination of 10 Hz and 20 μm gave the best quality measure for this combined characterization.

4. Concluding remarks

A novel in situ method allowing combined measurement of dimensional changes and mechanical properties during cure was presented in this work. These measurements were carried out in a single device called a thermal flux cell combined with a DMA. The resin is contained into a mold where its base and cover include heat flux sensors. This allows the monitoring of changes in temperature and thermal flux as well as the dynamical displacement and stiffness during cure. An epoxy DGEBA resin was used in this work to demonstrate the capability of this new approach. Different vibration frequencies and amplitude were used in order to optimize results as well as the quantity of resin. Optimum results were found for a mass of 1 g and application of 10 Hz frequency and 20 μm dynamical amplitude. The heat of reaction was found to be 337 J/g which is very close to the DSC value of 326 J/g. The averaged chemical linear shrinkage of the cured resin was of 2.5% and its stiffness reached a plateau of 10^7 N/m at the end of cure. The evolution of stiffness with the degree of cure was found to be nonlinear from the gelation point of 33%. The evolution of shrinkage with degree of cure was found to be linear from 54% cure up to 90% where the reaction starts being mostly controlled by diffusion.

Phenomenological models were also proposed to describe the shrinkage and stiffness behavior as a function of degree of cure. The shrinkage of the epoxy resin was modeled using a linear function of degree of cure. However, the initial cure at which shrinkage is noticeable was found to be higher than gelation point. The stiffness evolution was modeled using a log–log function that describes the increment of the dynamic mechanical properties with degree of cure. The proposed model and experimental data are in line with chemo and thermo-mechanical models found in the literature.

Acknowledgements

The authors acknowledge the support provided by the societies 01 dB Metravib and Thermoflux for their collaboration in the development of this innovative thermal flux cell. The authors thank the Natural Sciences and Engineering Research Council of Canada (NSERC) and the Canada Foundation for Innovation (CFI) for their financial support.

References

[1] Ruiz E. De la caractérisation des matériaux et simulation du procédé à l'optimisation de la fabrication des composites par injection sur renfort. Thèse de doctorat 2004. École Polytechnique de Montréal.
[2] Ruiz E, Trochu F. Numerical analysis of cure temperature and internal stresses in thin and thick RTM parts. Composites: Part A 2005;36(6):806–26.
[3] Hill RR, Shailesh JR, Muzumdar V, Lee LJ. Analysis of volumetric changes of unsaturated polyester resins during curing. Polym Eng Sci 1995;35(10):852–9.
[4] Li C, Potter K, Wisnom MR, Stringer G. In-situ measurement of chemical shrinkage of MY750 epoxy resin by a novel gravimetric method. Compos Sci Technol 2004;64(1):55–64.
[5] Holst M, Shanzlin K, Wenzel M, Xu J, Lellinger D, Alig I. Time-resolved method for the measurement of volume changes during polymerization. J Polym Sci 2005;43(17):2314–25.
[6] Yu H, Mhaisalkar SG, Wong EH. Cure shrinkage measurement of nonconductive adhesives by means of a thermomechanical analyzer. J Electron Mater 2005;34(8):1177–82.
[7] Causse P, Ruiz E, Trochu F. Thermoelastic spring-in of curved composite parts manufactured by flexible injection. Design, manufacturing and applications of composites. In: Proceedings of the eighth joint Canada-Japan workshop on composites; 2010. p. 313–23.
[8] Ramos JA, Pagani N, Riccardi CC, Borrajo J, Goyanes SN, Mondragon I. Cure kinetics and shrinkage model for epoxy–amine systems. Polymer 2005;46(10):3323–8.
[9] Boyard N, Millischer A, Sobotka V, Bailleul J-L, Delaunay D. Behavior of a moulded composite part: modelling of dilatometric curve (constant pressure) or pressure (constant volume) with temperature

and conversion degree gradients. Compos Sci Technol 2007;67(6):943–54.
[10] Khoun L, Hubert P. Cure shrinkage characterization of an epoxy resin system by two in situ measurement methods. Polym Compos 2010;31(9):1603–10.
[11] Eom Y, Boogh L, Michaud V, Sunderland P, Manson J-A. Stress-initiated void formation during cure of a three-dimensionally constrained thermoset resin. Polym Eng Sci 2001;41(3):492–503.
[12] Ruiz E, Trochu F. Thermomechanical properties during cure of glass-polyester RTM composites: elastic and viscoelastic modeling. J Compos Mater 2005;39(10):881–916.
[13] Schoch KF, Panackal PA, Frank PP. Real-time measurement of resin shrinkage during cure. Thermochim Acta 2004;417(1):115–8.
[14] Haider M, Hubert P, Lessard L. Cure shrinkage characterization and modeling of a polyester resin containing low profile additives. Composites: Part A 2007;38(3):994–1009.
[15] Ruiz E, Waffo F, Owens J, Billotte C, Trochu F. Modeling of resin cure kinetics for molding cycle optimization. In: The 8th international conference on flow processes in composite materials. Douai, France; 11–13 July 2006.
[16] Ruiz E, Billotte C. Predicting the cure of thermosetting polymers: the isoconversion map. Polym Compos 2008;30(10):1450–7.
[17] Danley RL. New heat flux DSC measurement technique. Thermochim Acta 2003;395(1–2):201–8.
[18] Reading M, Luget A, Wilson R. Modulated differential scanning calorimetry. Thermochim Acta 1994;238(15):295–307.
[19] Henne M, Breyer C, Niedermeier M, Ermanni P. A new kinetic and viscosity model for liquid composite molding simulations in an industrial environment. Polym Compos 2004;25(3):255–69.
[20] Bensadoun F, Kchit N, Billotte C, Trochu F, Ruiz E. A comparative study of dispersion techniques for nanocomposites made with nanoclays and unsaturated polyester resin. J Nanomater 2011;406087:12.
[21] Halley PJ, Mackay ME, George GA. Determining the gel point of an epoxy resin by various rheological methods. High Perfom Polym 1994;6:405–14.
[22] Winter HH. Can the gel point of a cross-linking polymer be detected by the G'–G'' crossover? Polym Eng Sci 1987;27(22):1698–702.
[23] Pascault JP, Williams RJJ. Relationships between glass transition temperature and conversion. Polym Bull 1990;24(1):115–21.
[24] Abou Msallem Y, Jacquemin F, Boyard N, Poitou A, Delaunay D, Chatel S. Material characterization and residual stresses simulation during the manufacturing process of epoxy matrix composites. Composites: Part A 2010;41(1):108–15.
[25] Lubin G. Handbook of composites. In: Peters ST, editor. 2nd ed. Springer-Verlag; 1998. p. 70–1.
[26] Hubert P, Poursartip A. A method for the direct measurement of the fibre bed compaction curve of composite prepregs. Composites Part A 2001;32(2):179–87.